JOURNAL OF VIROLOGY, June 1997, p. 4589–4598 Vol. 71, No. 6
0022-538X/97/$04.00+0

Bone Marrow Failure by Cytomegalovirus Is Associated with an In Vivo Deficiency in the Expression of Essential Stromal Hemopoietin Genes

ANNA MAYER,[1] JÜRGEN PODLECH,[1] SABINE KURZ,[1] HANS-PETER STEFFENS,[1] SABINE MAIBERGER,[1] KARIN THALMEIER,[2] PETER ANGELE,[3] LIANE DREHER,[3] AND MATTHIAS J. REDDEHASE[1]*

Institute for Virology, Johannes Gutenberg-University, 55101 Mainz,[1] Gesellschaft für Strahlenforschung, 81377 Munich,[2] and Department of Virology, University of Ulm, 89069 Ulm,[3] Germany

Received 8 November 1996/Accepted 26 February 1997

Bone marrow (BM) failure associated with cytomegalovirus (CMV) infection is a feared complication after clinical BM transplantation. Experiments in long-term BM cultures have indicated that BM stromal cells (BMSC) are targets of productive CMV infection, but an in situ infection of BM stroma remained to be documented, and the pathomechanism is open to question. Here we describe a murine in vivo model of lethal CMV aplastic anemia (CMV-AA). The reconstitution of hematopoietic progenitor cells expressing stem cell factor (SCF) receptor was found to be defective in CMV-AA. While murine CMV replication in permissive parenchymal tissues is cytolytic, the hematopoietic cord was found to be a site of very limited virus production with foci of reticular BMSC expressing the intranuclear viral IE1 protein, but with only a few BMSC positive for viral genome in the in situ hybridization. XX-XY BM chimeras were established in order to quantitate Y-chromosome-tagged BMSC by a PCR specific for the male-sex-determining gene *Tdy*. This approach revealed that murine CMV infection is not associated with a significant loss of BMSC. Despite the physical integrity of the stromal network, the functional integrity of the stroma was impaired. While housekeeping genes were expressed normally in BMSC of infected mice, the expression of genes encoding the essential hemopoietins SCF, granulocyte colony-stimulating factor, and interleukin-6 was markedly reduced. In conclusion, the mechanism of BM failure is not a stromal lesion but an insufficient stromal function. These findings explain CMV-AA as a manifestation of multiple hemopoietin deficiency.

In the period of immunodeficiency before the hematopoietic reconstitution by bone marrow (BM) transplantation becomes effective, primary or recurrent cytomegalovirus (CMV) can replicate cytolytically in multiple organs, with interstitial CMV pneumonia being known as the most severe manifestation of CMV disease (13, 30). There is increasing experimental (32, 36) as well as clinical (11, 14) evidence that a graft failure and consequent BM hypoplasia/aplasia due to an inhibition of hematopoiesis by CMV itself maintains the immunodeficient state and thus favors the development of multiple-organ CMV disease. In theory, CMV could inhibit hematopoiesis by targeting either of the two functional compartments of the BM (Fig. 1), namely, the hematopoietic compartment consisting of the pluripotent hematopoietic stem cells (PHSC) and their progeny in all hematopoietic lineages, and the supporting stromal compartment, which provides essential hemopoietins and the matrix necessary for homing, self-renewal, and differentiation of the PHSC (8, 44). Since CMV has a wide cell type tropism in vivo (33), these mechanisms are not mutually exclusive. However, infection of human CD34-positive early hematopoietic progenitor cells has been shown to result in a noncytopathic latency-like state that does not inhibit the generation of leukocytic progeny but generates a reservoir for the viral genome (23, 29, 31). In contrast, a deficiency in stromal functions would inhibit hematopoiesis at its earliest stage (reviewed in reference 9). Thus, an infection of the BM stroma provides the more likely explanation for BM aplasia. So far, evidence for a stromal failure caused by human as well as by murine CMV rests on the in vitro infection of the stromal layer of long-term BM cultures. This infection was found to be productive and eventually cytolytic. The cytopathic effect on stromal cells resulted in deprivation of essential hemopoietins and consequent cessation of the in vitro hematopoiesis (3, 7, 27, 28, 46). Does this straightforward explanation apply also to the BM failure in the infected host? The strict species specificity of CMV precludes an experimental in vivo study with human CMV, and therefore, the findings with respect to long-term BM cultures could not be validated for their relevance to human CMV pathogenesis. In this study, we have used the model system of murine CMV infection in its natural host, a model that has proven its predictive value for human CMV disease and for cytoimmunotherapy (38–40). In essence, the in vivo data presented here show that the prediction made by the in vitro experiments is only partially true in the host. BM stroma is indeed an in situ target of CMV infection. Interestingly, however, CMV exerts its adverse effects in the BM indirectly rather than directly, by inhibition of hemopoietin gene expression without significant cell destruction. This contrasts with the cytolytic, plaque-forming infection in permissive parenchymal tissues of organs. The findings document that a principally cytolytic virus can cause site-specific manifestations of disease by an alternative mechanism and explain CMV aplastic anemia (CMV-AA) as a consequence of a functional deficiency of the BM stroma.

* Corresponding author. Mailing address: Institute for Virology, Johannes Gutenberg University, Hochhaus am Augustusplatz, 55101 Mainz, Germany. Phone: 49-6131-173650. Fax: 49-6131-395604. E-mail: REDDEHAS@mzdmza.zdv.uni-mainz.de.

MATERIALS AND METHODS

Generation of XX-XY BM chimeras. Animal experiments were approved by the Ethic Commission, permission no. 177-07/941-4, according to German federal law. For the generation of BM chimeras, inbred mouse strain BALB/c (major histocompatibility complex [MHC] class I molecules K^d, D^d, and L^d) and

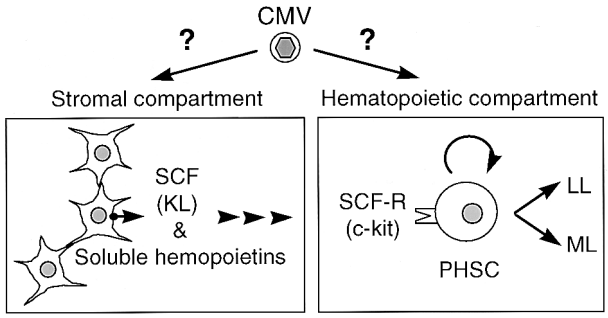

FIG. 1. Potential target compartments of CMV in early hematopoiesis. (Left box) Stromal compartment consisting of network-forming fibroblastoid RSC, adventitial reticular cells, and adipocytes in the hematopoietic cord. Stromal cells express membrane-bound SCF, also known as Kit ligand (KL), and secrete hemopoietins, such as soluble SCF, IL-6, and G-CSF. Arrowheads symbolize signalling. (Right box) Hematopoietic compartment consisting of the PHSC and all of its progeny in the lymphoid (LL) and myeloid (ML) lineages. The PHSC expresses SCF-R, a c-*kit*-encoded transmembranal tyrosine kinase. The curved arrow symbolizes the self-renewal capacity of the PHSC, and straight arrows symbolize differentiation into committed lineages.

the L^d-gene deletion mutant strain BALB/c-*H-2*^{dm2} (K^d and D^d only) were used at the age of 8 weeks for BM transplantation (BMT) as BM cell (BMC) donors and recipients. In either direction of BMT, recipients were males (XY genotype) and donors were females (XX genotype). For the hematoablative conditioning, recipients were total-body irradiated with a single dose of 8 Gy from a ^{137}Cs γ source (OB58; Buchler, Braunschweig, Germany) delivering a dose rate of ca. 0.7 Gy min^{-1} that was adjusted monthly. Donor femoral and tibial BMC were obtained as described previously (32), and 5×10^7 BMC were infused intravenously into the tail vein of recipients at ca. 6 h after the irradiation. The chimeras were used for the experiments 3 months later, that is, after a stable chimerism was established. The chimeric state was monitored by cytofluorometric analysis of MHC-L^d molecule cell surface expression. Mice were bred and housed under specific-pathogen-free conditions.

Infection of mice and assays of infectivity. If not indicated otherwise, experiments were performed with 8-week-old, female BALB/c mice. In the infection experiments, a sublethal irradiation with a dose of 6 Gy was chosen for the hematoablative treatment. This dosage allows for endogenous reconstitution of the BM in mice of the uninfected control group. Murine CMV, strain Smith ATCC VR-194, was purified by sucrose gradient ultracentrifugation as described previously (26), and mice were infected subcutaneously at the left hind footpad with 10^5 PFU at ca. 2 h after the irradiation. Titers of virus in organs were determined from the organ homogenates by a plaque assay on permissive second-passage mouse embryo fibroblasts (MEF), using the previously described (17, 26) technique of centrifugal enhancement of infectivity. Titers are expressed as PFU* to indicate the enhancement. Likewise, titers with no enhancement are expressed as PFU. Usually, for the calculation of the titer per organ, a $\log_{10}$ titration started with a 1/100 aliquot of an organ homogenate that was distributed to two cultures in flat-bottom 1-cm-diameter 48-well tissue culture plates (Falcon no. 3078; Becton Dickinson Labware, Franklin Lakes, N.J.) except for early times after infection, when 1/10 of the homogenate was tested. In the case of the BM, 1/10 of the homogenate of the BMC of one femur was plated throughout the kinetics, and the titer refers to one femur. This defines the detection limit of the plaque assay as 10 PFU*. For the quantitation of very low infectivity in the femoral BM of infected mice at day 14 after infection, the recently described reverse transcriptase PCR (RT-PCR)-based focus expansion assay was used (26). In brief, BMC were flushed quantitatively out of the femurs, frozen immediately at −70°C, subjected to Dounce homogenization at 4°C, and used in the indicated dilutions for the inoculation of close-to-confluence MEF in 10-cm-diameter petri dishes. To serve as a standard with defined infectivity, BMC recovered from femurs of uninfected mice at day 14 after a 6-Gy irradiation were supplemented with a defined dose of purified murine CMV expressed in terms of regular PFU, frozen, and processed accordingly. After centrifugal infection at $1{,}000 \times g$ and 72 h of focus formation in culture, poly(A)$^+$ RNA was isolated and a fragment of 188 bp specific for exons 3 and 4 of the murine CMV immediate-early (IE) gene *ie1* was amplified from 100 ng of the poly(A)$^+$ RNA by RT-PCR. Amplification products were analyzed by 2% (wt/vol) agarose gel electrophoresis, Southern blotting, and hybridization with an internal γ-^{32}P-end-labeled oligonucleotide probe directed against the splicing junction. Contaminating DNA can be distinguished by the size of the amplificate of 310 bp encompassing the intron. Specific signals were visualized by autoradiography using Kodak X-AR film.

Histological analysis. Histopathology in the BM and in adrenal glands was studied at day 14, which is close to the final stage of CMV disease in the lethally infected experimental group. Adrenal glands and femurs were fixed in 4% (vol/vol) formalin buffered at pH 7.4. In the case of the femurs, the bone substance was decalcified with either 20% (wt/vol) EDTA for subsequent hematoxylin-eosin (HE) staining as well as for in situ hybridization (ISH) or with 5% (wt/vol) trichloroacetic acid (TCA) for immunohistochemistry (IHC). Decalcification is a critical step, since ISH does not work after TCA treatment, whereas some unspecific staining is seen in the IHC after EDTA treatment. Paraffin sections of 2 μm were dewaxed in xylene and processed for HE staining according to established procedures.

For IHC, the intranuclear viral IE1 (pp89) protein (22) was detected by using monoclonal antibody (MAb) CROMA 101 (mouse immunoglobulin isotype G1; kindly provided by S. Jonjic, University of Rijeka, Rijeka Croatia) and an indirect avidin-biotin-peroxidase complex method (Vectastain ABC kit standard PK 4000; Vector Laboratories, Burlingame, Calif.) with diaminobenzidine for brown staining. Negative controls included uninfected tissue as well as replacement of the specific MAb CROMA 101 by murine immunoglobulin G1 as isotype control in the staining of infected tissue. For ISH, deparaffinized sections were subjected to digestion by 25 μg of RNase (DNase-free RNase no. 1119915; Boehringer, Mannheim, Germany) ml^{-1} for 30 min at 37°C, followed by 50 μg of proteinase K (no. P0390; Sigma) ml^{-1} for 20 min at 50°C. After washing with phosphate-buffered saline (PBS) and dehydration, sections were immersed with hybridization solution, which consisted of hybridization buffer (HybriBuffer ISH, no. R-012.050; Biognostik, Göttingen, Germany) containing, per ml, 1 μg of a digoxigenin-11-dUTP (DIG-dUTP)-labeled probe (PCR DIG probe synthesis kit, catalog no. 1636090; Boehringer) of 1,534 bp specific for the murine CMV gB gene sequence 5′-n313-1847, where n indicates nucleotide positions (35). Sections were covered with coverslips, which were then sealed with rubber cement. Denaturation was performed for 10 min at 93°C, followed by hybridization for 16 h at 32°C. After labeling for 1 h with alkaline phosphatase-conjugated anti-DIG antibody in the recommended dilution (no. 1093274; Boehringer), staining was performed with new fuchsin as the substrate, yielding a brilliant red. Counterstaining was done with hematoxylin. Negative controls included sections from uninfected tissue as well as omission of the hybridization probe in the staining of infected tissue.

Cytofluorometric analysis. Femoral plus tibial BMC were labeled with fluorescein isothiocyanate-conjugated MAbs specific for the MHC class I molecules L^d and D^d, clones 30-5-7S and 34-5-8S (Cedarlane, Hornby, Ontario, Canada), respectively. Measurements were performed with a FACSort (Becton Dickinson, San Jose, Calif.), using CellQuest software (Becton Dickinson) for data processing.

Relative quantitation of male cells by Y-chromosome-specific PCR. DNA was isolated from femoral plus tibial BMC by standard procedures of proteinase K digestion, phenol-chloroform-isoamyl alcohol extraction, and precipitation with ethanol. To increase the solubility, DNA was sonicated by using a Branson cup ultrasonicator (Branson Ultrasonics, Danbury, Conn.). A 402-bp DNA fragment of the male-sex-determining gene *Tdy* (16) was amplified in 35 cycles by using an MWG Biotech Hybaid OmniGene thermocycler (Hybaid Limited, Teddington, England) and AmpliTaq polymerase (Perkin-Elmer, Branchburg, N.J.). The reaction temperature profile was as follows: 1 min at 94°C for denaturation, 1 min at 52°C for annealing, and 1.5 min at 72°C for primer extension. Nucleotide positions of primers are indicated by counting from the 5′ terminus of the coding strand: forward primer, 5′-n70-89; reverse primer, 5′-n471-451. Amplification products (20-μl aliquots of the 100-μl reaction volumes) were separated on a 1.5% (wt/vol) agarose gel and visualized by autoradiography after Southern blotting and hybridization with the γ-^{32}P-end-labeled internal oligonucleotide probe 5′-n270-290 (16).

Analysis of gene expression by RT-PCR. Femoral and tibial BMC were sedimented at $600 \times g$ for 10 min, resuspended in PBS-A (PBS devoid of Ca^{2+} and Mg^{2+}), sedimented again, and dissolved in the extraction buffer of a QuickPrep-Micro mRNA purification kit (Pharmacia Biotech). Poly(A)$^+$ RNA was purified by an oligo(dT)-cellulose affinity method (4). Reverse transcription was performed with 100 U of Moloney murine leukemia virus RT (GIBCO BRL, Eggenstein, Germany) essentially as described previously (26). In brief, oligo(dT)-primer annealing was done for 10 min at 27°C, followed by reverse transcription for 30 min at 42°C and denaturation for 5 min at 95°C. A sample without addition of RT was routinely included to control for DNA contamination. The resulting cDNA was then amplified in 30 cycles (1 min at 94°C, 1 min at 65°C, and 1 min at 72°C) in a total volume of 50 μl, using 25 pmol of each primer and 1.5 U of AmpliTaq polymerase. Only in the case of c-*kit* was the amplification protocol modified to 1 min at 94°C for the denaturation, 2 min at 60°C for primer annealing, and 2 min at 72°C for the elongation. The verification of the amplification products was performed by Southern blot analysis and hybridization with the respective γ-^{32}P-end-labeled internal oligonucleotide probe, followed by autoradiography. For the relative quantitation of c-*kit* gene expression in BMC, radioactivity per band was measured as phosphodisintegrations with a digital phosphoimaging system (Phospho-Imager model GS 250; Bio-Rad). The primers (forward/reverse), probes, and fragment lengths were as follows: CMV-IE1, 5′-n1146-1170/n1522-1498, 5′-n1392-1418, 280 bp (21); CMV-gB, 5′-n2650-2669/n3034-3017, 5′-n2898-2917, 385 bp (35), GenBank accession no. M86302; HPRT (hypoxanthine phosphoribosyltransferase), 5′-n601-625/n763-739, 5′-n649-669, 163 bp (24), Swiss-Prot accession no. P00493; β-actin, 5′-n391-420/n1051-1022, 5′-n601-618, 661 bp (1), GenBank accession no. M12481; c-Kit (synonym, stem cell factor receptor [SCF-R]); 5′-n4480-4500/n5090-5070, 5′-n4947-4968, 611 bp (34), GenBank accession no. Y00864; stem

cell factor (SCF; synonym, Kit ligand), 5′-n223-250/n765-739, 5′-n695-716, 543 bp (2), GenBank accession no. M57647; granulocyte colony-stimulating factor (G-CSF), 5′-n134-155/n504-484, 5′-n269-292, 371 bp (48); GenBank accession no. MI3926; interleukin-6 (IL-6), 5′-n159-179/n677-655, 5′-n568-589, 519 bp (10), GenBank accession no. J03783.

RESULTS

Limited virus production in the BM during lethal multiple-organ CMV disease. It is a hallmark of human CMV infection that disease is restricted to the immunocompromised host. We have adapted the murine model of CMV infection for conforming to human CMV biology (39). Accordingly, intraplantar infection of immunocompetent, adult mice of the genetically susceptible inbred strain BALB/c (43) does not cause disease but generates protective antiviral T lymphocytes of the CD8 subset (for a review, see reference 25). The basic parameters of this model of murine CMV disease are represented by the experiment shown in Fig. 2. Hematoablative treatment by γ radiation leads to a dose-dependent mortality, and the dosage was adjusted so as to permit endogenous reconstitution of the BM and consequent high-rate survival. In contrast, in repeated experiments, all mice inevitably succumbed to multiple-organ disease between days 10 and 20 of a concurrent murine CMV infection, with the highest mortality around day 14 (Fig. 2, upper left). Day 14 was therefore selected as the time point for readout in all subsequent experiments. Titers of infectious virus in organs steadily increased during the observation period (Fig. 2, upper right). While virus replication in secretory glandular epithelial cells of the salivary glands is not associated with a marked histopathology (20), a viral pneumonia with widening of the alveolar septa is observed in the lungs (39). In the adrenal glands (37) and in the liver, the infection is cytolytic causing plaque-like tissue lesions. Previous work has implicated the BM in CMV pathogenesis, since lethal CMV disease was found to be associated with BM aplasia, measured then in terms of cellularity of the BM and numbers of early hematopoietic progenitor cells (32). It is therefore striking that the BM is apparently not a site of significant virus replication (Fig. 2, upper right). Since the titers of murine CMV in the BM of one femur were at the limit of detection of the plaque assay despite centrifugal enhancement of infectivity, we tested the homogenate of pooled yields of BMC by the recently described RT-PCR-based focus expansion assay in order to verify the presence of low amounts of infectious murine CMV in the BM with high sensitivity and accuracy. The focus expansion assay can detect infectivity in as few as ca. 0.01 PFU, which corresponds to five viral genomes (26). The assay involves centrifugal infection of permissive indicator cells in culture, formation of a focus during three rounds of viral replication, and detection of *ie1* transcripts in the infected cells by RT-PCR (26). As a standard for quantitation, a defined dose of purified CMV was added to femoral BMC recovered from the uninfected control group, and the homogenate thereof was titrated accordingly (Fig. 2, bottom). The fact that 0.01 PFU was clearly detected indicates that the procedure of homogenization did not diminish infectivity. In the infected group, infectivity was detected in a 1/100 aliquot of the yield of BMC of one femur (Fig. 2, center), which gives an estimate of ca. 100 infectious virions per femur. For verification, nine aliquots were tested, and seven of nine were found to be positive (not shown), which is in accordance with the Poisson statistics. However, this result cannot be taken as a formal proof for infection of the BM, because such a low dose of infectious virus could reflect the infection of intravasal leukocytic passengers within the femoral capillaries and sinusoids.

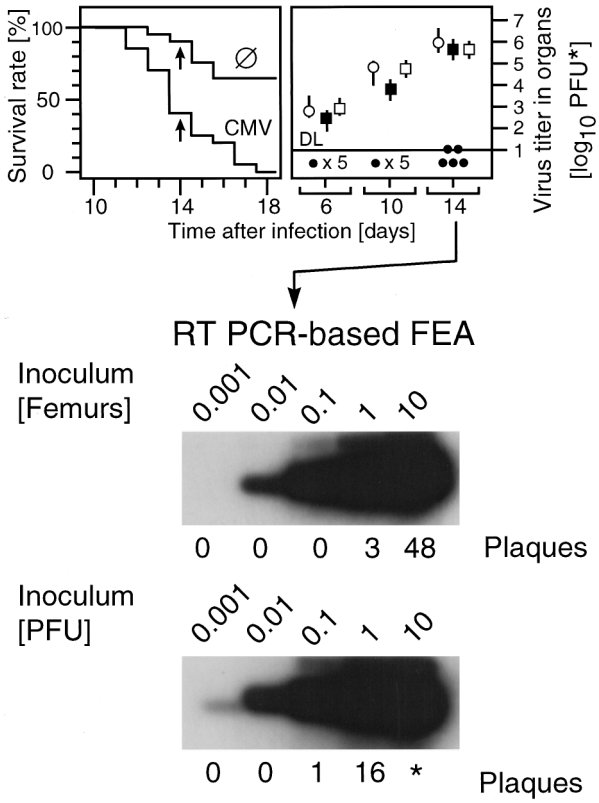

FIG. 2. Productivity of the infection in the course of lethal murine CMV disease. (Upper left) Kaplan-Meier survival plots showing the survival rates (ordinate) as a function of time after a sublethal γ irradiation with a dose of 6 Gy (abscissa) for groups of 20 mice. ∅, group with no infection. CMV, group with intraplantar murine CMV infection performed at day 0. The arrows mark the time point of maximal mortality chosen for the readout in subsequent experiments. (Upper right) Kinetics of virus replication in organs. Titers of virus in organ homogenates were determined by infection of indicator MEF with centrifugal enhancement and are expressed as PFU* to indicate the enhancement. DL, detection limit of 10 PFU*. Titers were determined individually for five mice per time point. For the sake of clarity, only the median value is depicted, and the range is indicated by a vertical bar. Symbols: open circles, salivary glands; solid circles, femoral BMC; solid squares, adrenal glands; open squares, lungs. (Center) High-sensitivity detection of infectivity by the RT-PCR-based focus expansion assay (FEA) (26). Dilutions of the homogenate of femoral BMC, corresponding to the indicated numbers of femurs recovered at day 14 from infected mice, were plated on MEF, and after 72 h of virus replication in the indicator cultures, 100 ng of poly(A)$^+$ RNA from each sample was subjected to *ie1* exon 3/4-specific RT-PCR. The autoradiographs shown were obtained after hybridization with a γ-^{32}P-end-labeled probe directed against the splice junction. The corresponding number of plaques in the cultures is indicated. (Bottom) As a standard for the quantitation, BMC recovered from the uninfected group were supplemented with a defined dose of purified virus and were processed and tested by RT PCR-based focus expansion assay accordingly. *, number of fusing plaques too high for an accurate counting.

Histological evidence for aplastic anemia and proof of the infection of reticular BMSC in the hematopoietic cord. Direct evidence for BM aplasia is provided by histological analysis of the BM (Fig. 3A and B). In the uninfected group, endogenous reconstitution of the BM with hematopoietic cells is visible at day 14 in the form of erythroblastic islands lining the endostal bone, the capillaries, and small vessels (Fig. 3A). Note the hemosiderin-containing central macrophage characteristic of an erythroblastic island (44). In other regions of a femoral section, analogous to the one shown, myelogranulopoietic islands were prominent as well. In contrast, simultaneous infection with murine CMV prevents such endogenous reconstitution. The histopathology in BM then ranges from severe

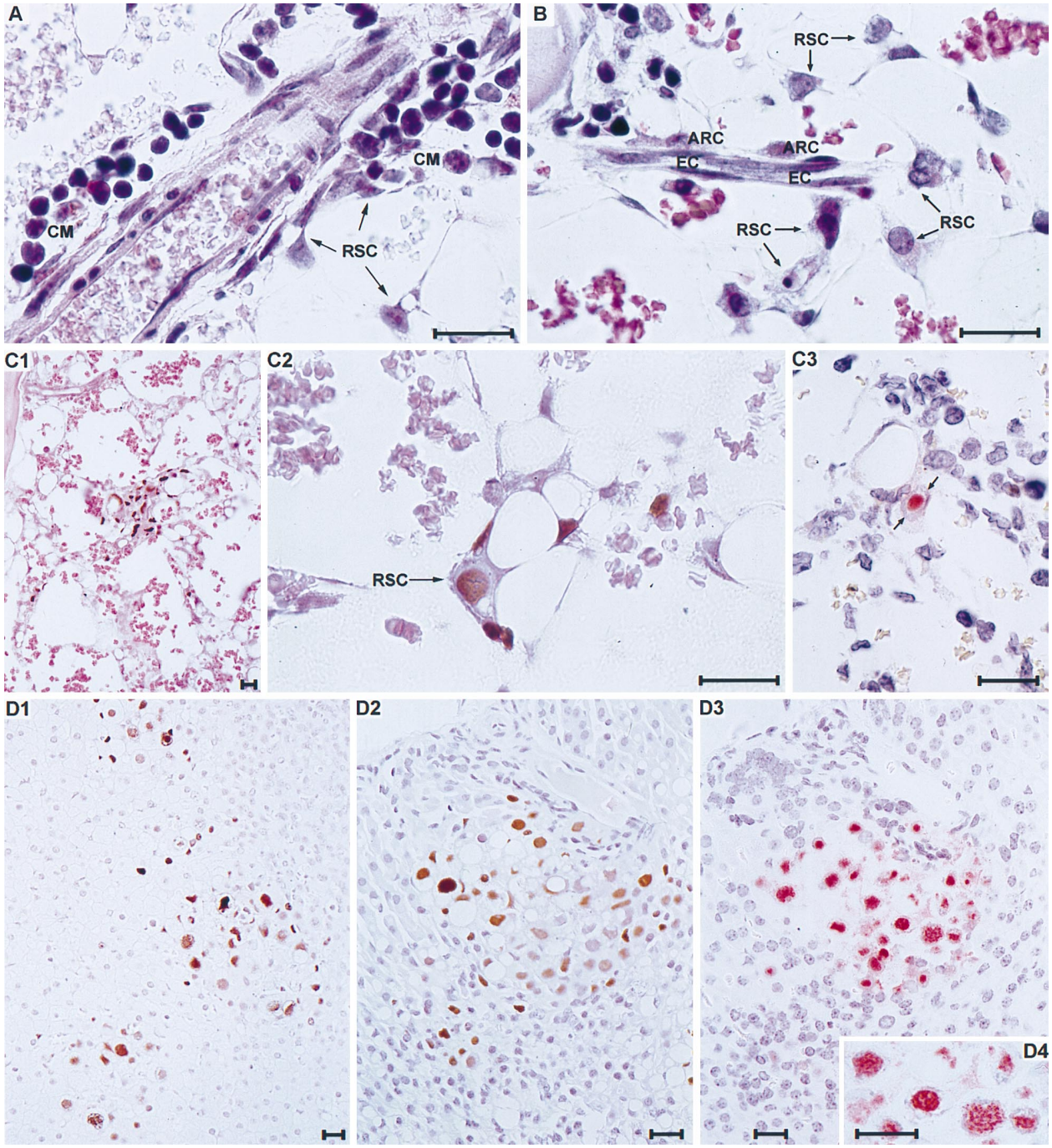

FIG. 3. Histological evidence for CMV-AA and localization of infected cells. (A) Endogenous reconstitution of BM visible by erythroblastic islands lining a small vessel in the diaphysial region of a femur at day 14 after a sublethal γ irradiation with 6 Gy (HE staining). Note the central macrophage (CM) characteristic of erythroblastic islands and fibroblastoid RSC in the hematopoietic cord (arrows). (B) BM hypoplasia to almost complete aplasia visible in an analogous section at day 14 after 6 Gy γ irradiation and intraplantar infection with murine CMV (HE staining). Note the empty but virtually intact stromal network formed by the interdigitating RSC. EC, endothelial cells of a capillary; ARC, adventitial reticular cells covering the endothelium's abluminal side. (C1 to C3) Detection of infected cells in femoral BM. (C1) Cluster of infected BMSC in the hematopoietic cord shown at low magnification in a longitudinal section of the diaphysis of a femur (IHC specific for the intranuclear viral IE1 protein [brown staining] with HE counterstaining). Note the condensed appearance of the stroma at the focus of infection. (C2) Group of infected RSC shown at greater detail, clearly revealing the intranuclear location of the IE1 protein. Note the virtual integrity of the cell-to-cell contacts. Staining is as in panel C1. (C3) A single infected BMSC detected by DNA-DNA ISH. The arrows mark the margin of the nucleus of the infected cell, where chromatin is condensed. The red-stained viral DNA is confined to the intranuclear inclusion body that is typically surrounded by a lucent, chromatin-free halo. The counterstaining was done with hematoxylin. (D1 to D4) Florid infection in the parenchyma of the adrenal gland cortex (AGC). (D1) Group of typical virus plaques in the AGC parenchyma, visualized by IHC specific for the viral IE1 protein (brown staining). The counterstaining was done with hematoxylin. (D2) A focus of infection at higher magnification. (IHC staining as in panel D1). Note the necrotic center of the plaque that is devoid of cell nuclei. (D3) Neighboring section in the same orientation and magnification as in D2, showing the same focus of infection by DNA-DNA ISH. Note the tissue invagination (upper right corner) that can serve as a landmark in D2 and D3. The counterstaining was done with hematoxylin. (D4) Detail of panel D3. Bars represent 20 μm throughout.

TABLE 1. Histological quantitation of murine CMV infection in AGC and femoral BM[a]

Organ	Measuring area[b] (mm^2)	No. of nucleated cells[c]	No. of IE1-positive cells[d]	No. of CMV DNA-positive cells[d]	% IE1-positive cells	% CMV DNA-positive cells	IE1-to-DNA-positive cell ratio
AGC	10	49,580	2,676	1,311	5.40	2.64	2.04
Femoral BM	100	137,700	214	13	0.16	0.01	16.46[e]
Ratio[f]	1.0[f]	3.6	125	1,008	34.8	293.8	

[a] Histological analysis (IHC and ISH) was performed at day 14 after infection. Data for the AGC were compiled from 18 sections derived from 18 adrenal glands of nine mice. Data for the femoral BM were compiled from 16 diaphysial sections derived from 16 femurs of eight mice. There was no difference in the extent of infection between left and right adrenal glands or between ipsilateral and contralateral femurs.

[b] The total measuring area was subdivided into 100 counting areas of 0.1 mm^2 for the AGC and into 200 counting areas of 0.5 mm^2 for the femoral BM.

[c] The number of nuclei was counted for 1 mm^2 of tissue and was extrapolated.

[d] Data represent absolute counts within the total measuring area. Note that the IE1 protein is detectable from the IE phase until the end of the viral replication cycle, whereas viral DNA located in the intranuclear inclusion body is indicative of cells in the late stage of the cycle.

[e] It is important to note that EDTA treatment, used for decalcification, has no influence on the sensitivity of ISH.

[f] Data for the AGC were extrapolated to a measuring area of 100 mm^2 and then divided by the data for the femoral BM.

hypoplasia to the almost complete aplasia as illustrated in Fig. 3B. Since this hypoplasia/aplasia is accompanied by pancytopenia of the peripheral blood (not shown), the model fulfills the definition of an aplastic anemia, and the disease manifestation is therefore referred to as CMV-AA. Notably, the radiation-resistant reticular stromal cells (RSC) in the hematopoietic cord did not show a morphologically evident cytopathic effect. They continued interdigitating with each other to form a virtually intact stromal network. Yet that the BM is principally an in situ target site of murine CMV is demonstrated by immunohistological analysis (Fig. 3C1 [overview] and C2 [detail]) that led to the detection of clusters of infected cells by staining of the intranuclear, regulatory viral IE1 protein. Notably, the stromal tissue at the focus of infection appears to be condensed rather than lysed to a plaque (Fig. 3C1). Viral replication in BM stromal cells (BMSC) is not, or at least not generally, arrested in the IE phase, since DNA-DNA ISH with a murine CMV gB gene-specific probe detected cells with a typical, viral DNA-containing intranuclear inclusion body that is characteristic of infected cells in a late stage of the viral replicative cycle (Fig. 3C3). Cell morphology (Fig. 3C2) and topographic location document that the infected cells in the aplastic BM are not residual hematopoietic cells, intravasal leukocytic passengers, or vasal endothelial cells but are in fact the RSC that make up the stromal network in the hematopoietic cord.

Histological quantitation of infected cells and indication of a delayed viral replication in the RSC of the BM. While foci of infection were detected in the BM stroma, the amount of infectious virus recovered from the BM was very low (Fig. 2). A low titer of virus could reflect a low number of infected cells, a low rate of productive infection, or a combination of both. It is therefore instructive to get a quantitative impression of the infection in the BM. For this, it is necessary not just to count the infected cells in the BM but to relate the result to the number of infected cells present at the same time in an organ with florid, cytolytic infection. We have chosen the adrenal gland cortex (AGC) as the reference tissue (Fig. 3D1 to D4). Immunohistology specific for the intranuclear viral IE1 protein, which is expressed from the IE phase throughout the viral replicative cycle, visualized typical three-dimensional virus plaques in the AGC (Fig. 3D1), with cell destruction in the center of advanced plaques and with infected cells at the plaque periphery. Serial, neighboring sections made it possible to document intranuclear IE1 protein expression and intranuclear presence of viral DNA for cells of the very same plaque (Fig. 3D2 and D3). In cells that are in the late stage of the viral replicative cycle, the viral DNA is concentrated in the intranuclear inclusion body (Fig. 3D4), which is the site of nucleocapsid assembly and viral DNA packaging (6, 49). Cells expressing IE1 and cells containing viral DNA were counted in sections of the AGC and the femoral BM and were related to the number of nucleated cells counted in the same areas (Table 1). It is worth noting that the number of nucleated cells per area is higher in the parenchymal tissue of the AGC than it is in the net-like BM stroma, a condition that favors the development of virus plaques in the AGC. The result lead to two interesting observations. First, the percentage of infected cells is much higher in the AGC, namely, 5.4% versus 0.16% on the basis of IE1-expressing cells. This was not unexpected in view of the low virus titer in the BM. At first glance, the percentage of infected cells during florid infection of the AGC also appears to be surprisingly low, but one has to consider that during cytolytic, plaque-forming infection, the extent of tissue damage is defined by the number of cells lysed and thus by the tissue area that is covered by plaques (Fig. 3D1). The second observation was not foreseeable: while in the AGC, half of the infected cells also carried late-phase inclusion bodies containing viral DNA, only 1/16 of the infected cells reached that state in the BM. Accordingly, on the basis of CMV DNA-positive cells per measuring area, the difference between AGC and BM is 1,000-fold. This finding indicates that virus replication is delayed in RSC of the BM, and most likely, the late phase will not be reached in most of the infected cells, because CMV disease is already in a final stage. In conclusion, the low virus production in the BM results from a low absolute number of infected cells and a low rate of productive infection.

Infection of BM stroma is not associated with a significant loss of BMSC. The conclusion drawn from the histology, namely, that infection does not cause extensive cell destruction in the BM stroma, was confirmed by an independent approach, designed for comparing the numbers of BMSC in infected and uninfected mice (Fig. 4). Cell counting is complicated by the fact that reconstituting hematopoietic cells are present in the uninfected BM (Fig. 3A) and that there exists no marker that would discriminate all types of BMSC from all types of hematopoietic cells. These technical problems were solved by performing the experiment with female-male BM chimeras, in which donor stem cells with the female XX genotype have repopulated recipient BM stroma of male XY genotype (Fig. 4A). A gene located on the Y chromosome, the male-sex-determining gene *Tdy* (16), served then as a substitute marker that specifies stromal cells. In addition, the expression of the MHC class I cell surface glycoprotein L^d in BALB/c mice and its absence in the deletion mutant BALB/c-H-2^{dm2} (41) was used to identify donor-derived hematopoietic cells positively

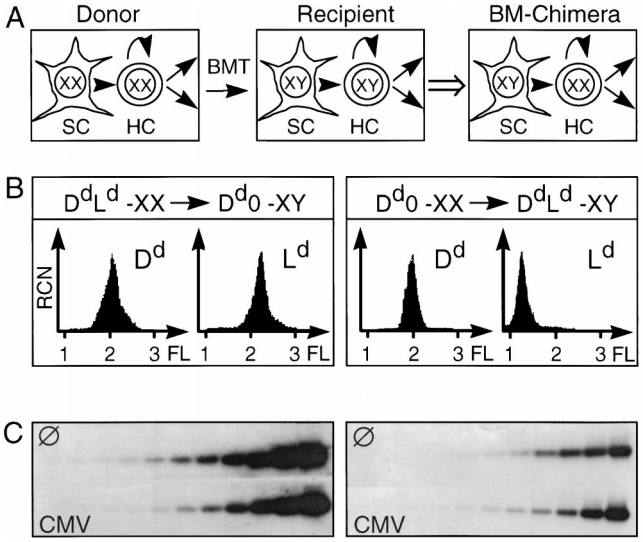

FIG. 4. Evidence against a loss of BMSC during lethal infection. (A) Design of the BMT for generating BM chimeras with female hematopoietic cells (HC) and male stromal cells (SC) carrying the male sex-determining gene *Tdy* on the Y chromosome as a tag. Symbols are as in Fig. 1. (B) Monitoring of the chimeric state. Cytofluorometric analysis of MHC class I glycoprotein D^d and L^d cell surface expression, demonstrating the XX-linked donor phenotype of the hematopoietic cells in the chimeras before the infection experiment was performed. Ordinate, relative cell number (RCN) with a total of 10,000 cells measured. Abscissa, $\log_{10}$ fluorescence (FL) intensity. (C) Relative quantitation of stromal cells by *Tdy* gene-specific PCR. DNA was recovered from five chimeras each of the uninfected (∅) and the infected (CMV) experimental group at day 14 after sublethal γ irradiation with a dose of 6 Gy. A $\log_2$ titration of DNA started with the yield of DNA equaling the BM stroma of one femur plus one tibia. Specific amplification products of 402 bp were visualized by autoradiography after Southern blot and hybridization with an internal probe.

(Fig. 4B, left) and negatively (Fig. 4B, right), respectively. The expression of MHC D^d in both strains provided the control. Cytofluorometric analysis proved that the hematopoietic cells in both types of chimeras were entirely of donor origin and thus of XX genotype. In consequence, the *Tdy* gene was exclusively present in recipient-derived, radiation-resistant BMSC. It should be noted that these cells are not visible by cytofluorometry of total BMC because of their low number. The question of whether donor-derived BMSC are transplantable by BMT is controversial (for a review, see reference 8). We have reinvestigated this question by using the XX-XY chimeras as BM donors and female mice as recipients, thus creating XX-XY-XX triple chimeras. A *Tdy* gene-specific PCR did not detect any male cells in the BM of the triple chimeras (not shown), which implies that under the conditions used here, donor BMSC were not transplanted. Three months after setting up the XX-XY chimeras, that is, when a stable chimerism was established, we performed the infection experiment. Endpoint titration of the femoral and tibial yields of DNA followed by *Tdy* gene-specific PCR documented that the number of BMSC was not significantly reduced by the infection (Fig. 4C), irrespective of which of the two mouse strains was the donor and which was the recipient.

Infection prevents the endogenous reconstitution of hematopoietic cells expressing SCF-R. With the exception of rare foci of infection with condensed stromal tissue (Fig. 3C1), the stromal network did not show a histopathic effect. In face of this morphological integrity, attention was turned to the functional properties of the BM stroma. The interaction between SCF-R (synonyms, CD117 and c-Kit), a transmembranal tyrosine kinase expressed by hematopoietic progenitors, and its counterreceptor SCF (Kit ligand), expressed by BMSC, is a decisive molecular event in the initiation of hematopoiesis (reviewed in references 8 and 50) (Fig. 1). Accordingly, if BMSC are deficient in providing the SCF signal, SCF-R-expressing hematopoietic stem and progenitor cells should fail to proliferate, with consequent BM aplasia. While histology can document aplasia by the gross absence of a progeny (Fig. 3B), a quantitation of SCF-R gene expression in BMC will show specifically whether the block in reconstitution already affects SCF-R-positive early stem and progenitor cells, which make up only 5 to 10% of the hematopoietic cells in normal BM (19). It is worth noting that the murine CD34 analog, unlike human CD34, is not an exclusive marker for early hematopoietic progenitors but is expressed also by stromal cells types (5). CD34 can therefore not substitute for CD117 in the analysis of murine hematopoiesis. To serve as a reference for the quantitation, SCF-R gene expression in BMC of normal, femoral, and tibial BM was determined by poly(A)$^+$ RNA dilution followed by RT-PCR (Fig. 5, reference row R). Endogenous reconstitution of radiation-sensitive SCF-R-expressing hematopoietic stem- and progenitor cells was monitored accordingly at day 14 after a sublethal γ irradiation with a single dose of 6 Gy (group

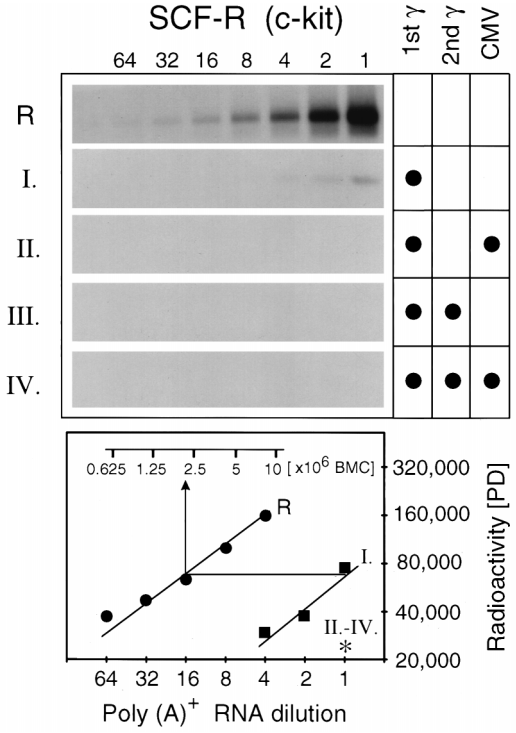

FIG. 5. Abrogation of endogenous hematopoietic reconstitution. The expression of SCF-R mRNA in BMC was quantitated at day 14 by endpoint dilution of poly(A)$^+$ RNA followed by SCF-R-specific RT-PCR. The poly(A)$^+$ RNA was recovered from five mice per group. A $\log_2$ titration started with the yield of poly(A)$^+$ RNA equaling the BMC content of one femur plus one tibia. (Top) The experimental regimen is indicated for normal BM taken as a reference (R) and for experimental groups I to IV. 1st γ, γ irradiation with a dose of 6 Gy performed at day 0; 2nd γ, γ irradiation with a dose of 7 Gy performed at day 13; CMV, intraplantar infection with murine CMV at day 0. Specific amplification products of 611 bp were visualized by autoradiography after Southern blot and hybridization with an internal γ-^{32}P-end-labeled probe. (Bottom) Computed phosphoimaging results of the same Southern blots. Log-log plots of phosphodisintegrations per band (PD; ordinate) versus the poly(A)$^+$ RNA dilutions (abscissa) are shown. The internal ruler relates the dilutions to the numbers of BMC in normal BM. Note that the number of BMC in experimental groups I to IV was too low for an accurate counting. *, values did not exceed the background of 20,000 PD.

I). At this early time point after the hematoablative treatment, reconstitution was not yet completed. Quantitation by phosphoimaging showed a 16-fold difference in the expression of SCF-R between normal BM and reconstituting BM, with the expression in the reconstituting BM corresponding to the expression in ca. 2×10^6 BMC of normal BM. This number represents a maximum estimate, since the expression of SCF-R is likely to be enhanced during reconstitution. The result of the quantitation is in good accordance with the histological visualization of the reconstituting BM, in which hematopoiesis at day 14 was still confined to hematopoietic islands (Fig. 3A). Likewise, the aplasia seen at day 14 after infection (Fig. 3B) has its molecular correlate in the complete absence of SCF-R expression (Fig. 5, group II). In conclusion, the inhibition of hematopoiesis by murine CMV operates early in hematopoiesis and affects the reconstitution of SCF-R-expressing hematopoietic stem and progenitor cells.

Selective deficiency in stromal hemopoietin gene expression. Since the membrane-bound form of SCF is the counterreceptor of SCF-R (12), a deficient expression of SCF by stromal cells could provide a straightforward explanation for reduced reconstitution of SCF-R-expressing hematopoietic stem and progenitor cells. To test this hypothesis, cytokine gene expression must be analyzed in stromal cells. For cytokines that are expressed exclusively in BMSC, as is the case with SCF, expression in the infected group could be compared directly with expression in the reconstituting group. However, for cytokines expressed in stromal cells and in hematopoietic cells, as is the case with IL-6 (45), reconstituting hematopoietic cells in the uninfected group would obscure the comparison of stromal gene expression. This technical problem was solved by a second γ irradiation of the mice with a dose of 7 Gy performed on the day before the analysis. That this treatment abrogated transcription in radiation-sensitive hematopoietic cells is documented by the absence of SCF-R message in the BM of uninfected mice (Fig. 5, group III). To account for effects of the second irradiation, the infected mice were also irradiated twice (Fig. 5, group IV), and analysis of stromal cytokine mRNA was performed as a comparison between groups III and IV by endpoint titration of the yields of poly(A)$^+$ RNA of one femur plus one tibia followed by RT-PCR specific for the indicated genes (Fig. 6). In accordance with the immunohistology (Fig. 3C1 and C2), expression of the *ie1* gene was also documented on the transcriptional level. In accordance with the ISH (Fig. 3C3), transcripts from the gB gene, a gene expressed in the late phase of the CMV replicative cycle (35), demonstrated that at least some infected cells proceeded to the late phase. Notably, in accordance with the result of the stromal *Tdy* gene quantitation in the XX-XY BM-chimeras (Fig. 4), expression of the housekeeping genes encoding HPRT and β-actin was not reduced by the infection. This finding excluded an unspecific, general inhibition of stromal gene expression and provided further evidence for a physical integrity of the BM stroma. This raised the question of whether the stroma was impaired at all by the infection. We then tested the expression of genes that encode hemopoietins essential for the functional integrity of the BM stroma. As we had reasoned from the lack of SCF-R-expressing hematopoietic cells, SCF expression should be affected, and indeed, mRNA encoding SCF was found to be markedly reduced in the BM stroma of infected mice. Yet the adverse effect of infection, whatever the molecular mechanism may be, was not restricted to SCF gene expression, since the expression of G-CSF and that of IL-6 were found to be reduced correspondingly.

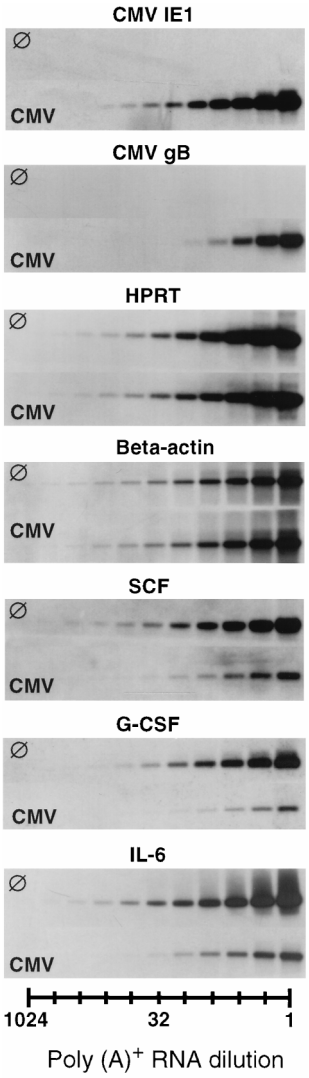

FIG. 6. Multiple deficiency in stromal hemopoietin gene expression. The analysis of gene expression was experimentally restricted to BMSC by the strategy of repeated irradiation outlined in Fig. 5. Starting with the yield equaling the BM stroma of one femur plus one tibia, poly(A)$^+$ RNA recovered from 10 mice each of the uninfected (∅; corresponding to group III in Fig. 5) and the infected (CMV; corresponding to group IV in Fig. 5) experimental group was titrated in $\log_2$ steps followed by RT-PCR specific for the indicated genes. Specific amplification products were visualized by autoradiography after Southern blot and hybridization with the respective internal probes.

DISCUSSION

The first experimental in vivo evidence for a BM aplasia caused by CMV was provided by the work of Mutter et al. (32). In a BALB/c murine model system, it was documented that endogenous reconstitution of hematopoiesis after a sublethal hematoablative treatment is interrupted by CMV infection after an initial onset. This conclusion was drawn from the kinetics of the cellularity of the BM and from the quantitation of progenitor cells of the myeloid hematopoietic lineage by colony-forming progenitor cell assays. A cellular target of CMV infection in the BM was not identified then, but the observed failure in the regeneration of the pool of myeloid progenitors had already implied that CMV pathogenesis in the BM operates at an early stage of hematopoiesis by affecting either the stem or progenitor cells directly or by affecting the stromal

compartment that is essential for their homing, self-renewal, and differentiation.

To this knowledge, the present work adds the histological visualization of the hematopoietic reconstitution in the uninfected group as well as of the aplasia in the infected group, and it dates the failure in reconstitution to a stage in the hematopoietic differentiation hierarchy at or before the renewal of the SCF-R-positive stem and progenitor cells. As illustrated in Fig. 1, a reduced self-renewal capacity of the SCF-R-expressing cells could result from an effect of CMV on the hematopoietic compartment itself, that is, in the easiest assumption, from infection of the progenitor cells. Alternatively, the proliferation of SCF-R-expressing progenitors could be limited by a lack of stromal support caused by infection of the BMSC. Our interest was focused on the BM stroma, since previous work has demonstrated that progenitor cells derived from infected BM or from an infected BMC culture continue normal proliferation and differentiation after a rescue transfer to a healthy stromal microenvironment (7, 15, 32). By contrast, the yield of stromal fibroblast colonies in cultures of BMC derived from infected mice was found to be reduced (47). Collectively, these results have clearly pointed to the stromal compartment of the BM as the principal target site of CMV pathogenesis.

Experiments of the present work have addressed two possible mechanisms of CMV pathogenesis in the BM stroma: first, a cytolytic infection of stromal cells and, second, the induction of a functional deficiency of stromal cells. A destructive, cytolytic infection of fibroblast-like BMSC appeared to be the most plausible pathomechanism for a virus that is known to form plaques in monolayers of fibroblasts. Several studies, our own previous work included, have demonstrated that stromal cells are the principal targets of productive CMV infection in long-term BM cultures. This was true not only for murine CMV (7) but also for the human CMV laboratory strain AD169 (3) and, most importantly, also for the majority of human CMV clinical isolates (46). Because of the slow replication cycle of human CMV, a decline in hemopoietin expression was observed as a functional cytopathic effect preceding cytolysis (27, 28, 46). It was therefore concluded that a disturbed hemopoietin expression is the mechanism of BM failure in long-term BM cultures, and it was speculated that this explanation may apply also to CMV pathogenesis in the immunocompromised host.

We have here established an in vivo model of CMV-AA to address the central question relevant to the mechanism of CMV pathogenesis in the BM, namely, is the hematopoietic cord a tissue site of CMV infection? Surprisingly, even during lethal infection with multiple organ involvement, the virus titer in the BM was close to the detection limit of the PFU assay, and only the recently described RT-PCR-based focus expansion assay (26) gave an estimate of ca. 100 infectious virions per femoral BM. This finding is in disagreement with work of Yuhasz et al. (51), who have reported an infection of the BM from a significant virus titer detected by a standard PFU assay shortly after intravenous infection of mice with murine CMV. However, infectivity detected in vitro in a suspension of BMC could result from free virions or from infected leukocytes floating in the capillaries and sinusoids of the BM. This objection also applies to the low infectivity detected in our experiments. Histological analysis is therefore imperative before any conclusion on an infection of the hematopoietic cord can be made. Immunohistological detection of the intranuclear viral IE1 protein and the ISH detecting viral DNA in intranuclear inclusion bodies unequivocally identified the stromal network-forming RSC of the hematopoietic cord as target cells of murine CMV infection within the BM. Yet the second finding is that the number of infected RSC is very low. Compared with the florid infection of a permissive tissue, such as the parenchyma of the AGC, the number of IE1-expressing cells per unit area of the section was 125-fold higher in the permissive reference tissue, and on the basis of CMV DNA-positive cells, the difference increased to 1,000-fold. Interestingly, the ratio between cells in the late phase of the viral replication cycle, as signified by a viral DNA-positive intranuclear inclusion body, and all infected cells, as signified by intranuclear IE1 protein, was 1:2 in the permissive tissue and only 1:16 in the BM. Apparently, infection in the RSC of the BM has difficulties in proceeding to the late phase. This finding does not necessarily imply that the infection is abortive in a high percentage of the RSC. Alternatively, it could reflect a delayed replication cycle, which was not yet completed at the time of analysis. When extrapolated to the volume of a femur of ca. 3.5 mm^3, the average number of viral DNA-positive cells per femur was ca. 100. As the estimated number of infectious virions was also 100, the ratio of one virion per DNA-positive cell suggests that at the time of analysis, only a minority of the DNA-positive cells contained mature virions. In accordance with this very low productivity, the infection did not destroy a significant proportion of the RSC, as evidenced by (i) the integrity of the stromal architecture in large areas of the femoral BM, (ii) the unchanged number of *Tdy*-gene positive stromal cells in the female-male BM chimeras, and (iii) the unchanged expression of the housekeeping genes encoding HPRT and β-actin. A one-to-one replacement of infected stromal cells could be thought of as an alternative explanation for the data. However, the histology did not give an indication of a regenerative process in the infected stroma, and the low virus productivity also argues against a dynamic model of cytolytic stroma cell infection and renewal. Altogether, these findings exclude an extensive cytolytic infection of the BM stroma as the mechanism of in vivo BM failure.

Instead, the markedly reduced expression of the essential stromal hemopoietins SCF, G-CSF, and IL-6 is clearly indicative of deficient stromal function. One might speculate that cytolytic infection may hit a minor subset of stromal cells expressing these cytokines and that an elimination of this subset would be invisible in the histology and in the *Tdy* gene assay. In fact, in the case of IL-6, the frequency of secreting cells determined by a very sensitive ELIspot assay is only 0.5% of the BMC in normal BALB/c BM (45), and the main producers are macrophages, that is, descendants of the myeloid hematopoietic lineage. It is therefore instructive to note that with the sensitivity of our RT-PCR, IL-6 mRNA was not detected within the excess of unrelated poly(A)$^+$ RNA of BMC from normal BM. Thus, the IL-6 mRNA detected during reconstitution and during CMV-AA is derived from radiation-resistant producers that were relatively enriched in the BM by the elimination of the radiation-sensitive majority of the BMC. Accordingly, we cannot formally exclude that the IL-6 mRNA was derived from few radiation-resistant macrophages rather than from a large number of BMSC. However, this argument does not apply to SCF. Its mRNA is also undetectable in unseparated BMC, but it is expressed selectively in stromal cells and there in basically all stromal cell types. It appears to us very unlikely that a minor subset of stromal cells would quantitatively account for the mRNA of three different hemopoietins and simultaneously represent the cell type that is permissive for CMV infection. Even more unlikely, the postulated minor subset must be proposed to be arranged in clusters within the stromal network, as infected cells were always seen in clusters (Fig. 3C1). Altogether, we conclude that the reduction in hemopoietin gene expression is not explained by a direct, cytolytic or noncytolytic, infection of the expressing stromal cells.

As a consequence, we have now to propose an indirect mechanism that is apparently induced by the infection but is operative mainly on uninfected bystander stromal cells. This could be the induction of a negative regulator of hemopoietin gene expression or, alternatively, the repression of a positive regulator. We presently only know that the mechanism is selective in that it affects only the highly regulated hemopoietin gene expression, not the expression of housekeeping genes. It is therefore not a general toxic effect. It is, however, not specific for a particular hemopoietin gene. At first glance, this aspect of our work appears to contradict previous work by Simmons et al. (46), who have concluded that human CMV infection of BMSC results in a specific deficiency of G-CSF transcripts. Yet this conclusion was based on an analysis of granulocyte-macrophage colony-stimulating factor, macrophage colony-stimulating factor, and G-CSF transcription, not including SCF and IL-6. Thus, our data add the important information that CMV infection does not exclusively affect G-CSF transcription. It must be emphasized that our present in vivo experiments were not designed to discriminate between transcription rate and transcript stability.

One might argue that more cytokines should be analyzed to get the full picture. Yet considering the hierarchy of hemopoietins, it is evident that a deficiency in first-order stromal hemopoietins resulting in BM aplasia will affect secondary hemopoietins. The reduced expression of the first-rank stromal hemopoietin SCF, which is encoded at the Steel locus (SL) (52), certainly contributes to the observed clinical phenotype of CMV-AA. Homozygous SL/SL mutant mice die in utero with anemia, and an allelic form of the Steel mutation resulted in the viable but severely anemic SL/SL^{d} strain (42). This demonstrates the significance of SCF in hematopoiesis. However, CMV-AA is more than a viral Steel syndrome, since deficient expression of G-CSF, IL-6, and possibly yet to be identified other cytokines/hemopoietins is likely to add to the disease phenotype in the BM. The role of G-CSF in granulopoiesis is evident, and IL-6 has been implicated in the proliferation of multipotential hematopoietic progenitors as a factor operating in synergy with IL-3 (18). In the case of SCF, the main function in hematopoiesis is mediated not by the soluble form but by the membrane-bound form (12). For this reason, and also because more than one hemopoietin is involved, application of soluble recombinant hemopoietins is not a promising approach for a therapy of CMV-AA.

ACKNOWLEDGMENTS

We thank Doris Dreis and Susanne Schmalz for expert technical assistance and Wenceslao Calvo, Department of Clinical Physiology, University of Ulm, Ulm, Germany, for advice in the interpretation of the BM histopathology.

This work was supported by a grant to M.J.R. by the Deutsche Forschungsgemeinschaft, Sonderforschungsbereich 311.

REFERENCES

1. **Alonso, S., A. Minty, Y. Bourlet, and M. Buckingham.** 1986. Comparison of three actin-coding sequences in the mouse; evolutionary relationships between the actin genes of warm-blooded vertebrates. J. Mol. Evol. **23:**11–22.
2. **Anderson, D. M., S. D. Lyman, A. Baird, J. M. Wignall, J. Eisenman, C. Rauch, C. J. March, H. S. Boswell, S. D. Gimpel, D. Cosman, and D. E. Williams.** 1990. Molecular cloning of mast cell growth factor, a hematopoietin that is active in both membrane bound and soluble forms. Cell **63:**235–243.
3. **Apperley, J. F., C. Dowding, J. Hibbin, J. Buiter, E. Matutes, P. J. Sissons, M. Gordon, and J. M. Goldman.** 1989. The effect of cytomegalovirus on hematopoiesis: in vitro evidence for selective infection of marrow stromal cells. Exp. Hematol. **17:**38–45.
4. **Badley, J. E., G. A. Bishop, T. St. John, and J. A. Frelinger.** 1988. A simple, rapid method for the purification of poly A+ RNA. BioTechniques **6:**114–116.
5. **Baumhueter, S., N. Dybdal, and L. A. Lasky.** 1994. Global vascular expression of murine CD34, a sialomucin-like endothelial ligand for L-selectin. Blood **84:**2554–2565.
6. **Bühler, B., G. M. Keil, F. Weiland, and U. H. Koszinowski.** 1990. Characterization of the murine cytomegalovirus early transcription unit e1 that is induced by immediate-early proteins. J. Virol. **64:**1907–1919.
7. **Busch, F. W., W. Mutter, U. H. Koszinowski, and M. J. Reddehase.** 1991. Rescue of myeloid lineage-committed preprogenitor cells from cytomegalovirus-infected bone marrow stroma. J. Virol. **65:**981–984.
8. **Chabannon, C., and B. Torok-Storb.** 1992. Stem cell-stromal cell interactions. Curr. Top. Microbiol. Immunol. **177:**123–136.
9. **Childs, B., and D. Emanuel.** 1993. Cytomegalovirus infection and compromise. Exp. Hematol. **21:**198–200. (Editorial.)
10. **Chiu, C. P., C. Moulds, R. L. Coffman, D. Rennick, and F. Lee.** 1988. Multiple biological activities are expressed by a mouse interleukin 6 cDNA clone isolated from bone marrow stromal cells. Proc. Natl. Acad. Sci. USA **85:**7099–7103.
11. **Einsele, H., G. Ehninger, M. Steidle, I. Fischer, S. Bihler, F. Gerneth, A. Vallbracht, H. Schmidt, H. D. Waller, and C. A. Müller.** 1993. Lymphocytopenia as an unfavorable prognostic factor in patients with cytomegalovirus infection after bone marrow transplantation. Blood **82:**1672–1678.
12. **Flanagan, J. G., D. C. Chan, and P. Leder.** 1991. Transmembrane form of the kit ligand growth factor is determined by alternative splicing and is missing in the Sld mutant. Cell **64:**1025–1035.
13. **Forman, S. J., and J. A. Zaia.** 1994. Treatment and prevention of cytomegalovirus pneumonia after bone marrow transplantation: where do we stand? Blood **83:**2392–2398.
14. **Fries, B. C., D. Khaira, M. S. Pepe, and B. Torok-Storb.** 1993. Declining lymphocyte counts following cytomegalovirus (CMV) infection are associated with fatal CMV disease in bone marrow transplant patients. Exp. Hematol. **21:**1387–1392.
15. **Gibbons, A. E., P. Price, and G. R. Shellam.** 1995. Analysis of hematopoietic stem and progenitor cell populations in cytomegalovirus-infected mice. Blood **86:**473–481.
16. **Gubbay, J., J. Collignon, P. Koopman, B. Capel, A. Economou, A. Münsterberg, N. Vivian, P. Goodfellow, and R. Lovell Badge.** 1990. A gene mapping to the sex-determining region of the mouse Y chromosome is a member of a novel family of embryonically expressed genes. Nature **346:**245–250.
17. **Hudson, J. B., V. Misra, and T. R. Mosmann.** 1976. Cytomegalovirus infectivity: analysis of the phenomenon of centrifugal enhancement of infectivity. Virology **72:**235–243.
18. **Ikebuchi, K., G. G. Wong, C. G. Clark, J. N. Ihle, Y. Hirai, and M. Ogawa.** 1987. Interleukin 6 enhancement of interleukin 3-dependent proliferation of multipotential hemopoietic progenitors. Proc. Natl. Acad. Sci. USA **84:**9035–9039.
19. **Ikuta, K., and I. L. Weissman.** 1992. Evidence that hematopoietic stem cells express mouse c-kit but do not depend on steel factor for their generation. Proc. Natl. Acad. Sci. USA **89:**1502–1506.
20. **Jonjic, S., W. Mutter, F. Weiland, M. J. Reddehase, and U. H. Koszinowski.** 1989. Site-restricted persistent cytomegalovirus infection after selective long-term depletion of CD4^{+} T lymphocytes. J. Exp. Med. **169:**1199–1212.
21. **Keil, G. M., A. Ebeling-Keil, and U. H. Koszinowski.** 1987. Sequence and structural organization of murine cytomegalovirus immediate-early gene 1. J. Virol. **61:**1901–1908.
22. **Keil, G. M., M. R. Fibi, and U. H. Koszinowski.** 1985. Characterization of the major immediate-early polypeptides encoded by murine cytomegalovirus. J. Virol. **54:**422–428.
23. **Kondo, K., H. Kaneshima, and E. S. Mocarski.** 1994. Human cytomegalovirus latent infection of granulocyte-macrophage progenitors. Proc. Natl. Acad. Sci. USA **91:**11879–11883.
24. **Konecki, D. S., J. Brennand, J. C. Fuscoe, C. T. Caskey, and A. C. Chinault.** 1982. Hypoxanthine-guanine phosphoribosyltransferase genes of mouse and Chinese hamster: construction and sequence analysis of cDNA recombinants. Nucleic Acids Res. **10:**6763–6775.
25. **Koszinowski, U. H., M. Del Val, and M. J. Reddehase.** 1990. Cellular and molecular basis of the protective immune response to cytomegalovirus infection. Curr. Top. Microbiol. Immunol. **154:**189–220.
26. **Kurz, S., H.-P. Steffens, A. Mayer, J. R. Harris, and M. J. Reddehase.** 1997. Latency versus persistence or intermittent recurrences: evidence for a latent state of murine cytomegalovirus in the lungs. J. Virol. **71:**2980–2987.
27. **Lagneaux, L., A. Delforge, R. Snoeck, E. Bosmans, D. Schols, E. DeClercq, P. Stryckmans, and D. Bron.** 1996. Imbalance in production of cytokines by bone marrow stromal cells following cytomegalovirus infection. J. Infect. Dis. **174:**913–919.
28. **Lagneaux, L., A. Delforge, R. Snoeck, P. Stryckmans, and D. Bron.** 1994. Decreased production of cytokines after cytomegalovirus infection of marrow-derived stromal cells Exp. Hematol. **22:**26–30.
29. **Maciejewski, J. P., E. E. Bruening, R. E. Donahue, E. S. Mocarski, N. S. Young, and S. C. St. Jeor.** 1992. Infection of hematopoietic progenitor cells by human cytomegalovirus. Blood **80:**170–178.
30. **Meyers, J. D., N. Flournoy, and E. D. Thomas.** 1986. Risk factors for cyto-

megalovirus infection after human marrow transplantation. J. Infect. Dis. **153:**478–488.
31. **Minton, E. J., C. Tysoe, J. H. Sinclair, and J. G. Sissons.** 1994. Human cytomegalovirus infection of the monocyte/macrophage lineage in bone marrow. J. Virol. **68:**4017–4021.
32. **Mutter, W., M. J. Reddehase, F. W. Busch, H. J. Bühring, and U. H. Koszinowski.** 1988. Failure in generating hematopoietic stem cells is the primary cause of death from cytomegalovirus disease in the immunocompromised host. J. Exp. Med. **167:**1645–1658.
33. **Plachter, P., C. Sinzger, and G. Jahn.** 1996. Cell types involved in replication and distribution of human cytomegalovirus. Adv. Virus Res. **46:**195–261.
34. **Qiu, F., P. Ray, K. Brown, P. E. Barker, S. Jhanwar, F. H. Ruddle, and P. Besmer.** 1988. Primary structure of c-kit: relationship with the CSF-1/PDGF receptor kinase family. EMBO J. **7:**1003–1011.
35. **Rapp, M., M. Messerle, B. Bühler, M. Tannheimer, G. M. Keil, and U. H. Koszinowski.** 1992. Identification of the murine cytomegalovirus glycoprotein B gene and its expression by recombinant vaccinia virus. J. Virol. **66:** 4399–4406.
36. **Reddehase, M. J., L. Dreher-Stumpp, P. Angele, M. Balthesen, and M. Susa.** 1992. Hematopoietic stem cell deficiency resulting from cytomegalovirus infection of bone marrow stroma. Ann. Hematol. **64**(Suppl. A)**:**A125–A127.
37. **Reddehase, M. J., S. Jonjic, F. Weiland, W. Mutter, and U. H. Koszinowski.** 1988. Adoptive immunotherapy of murine cytomegalovirus adrenalitis in the immunocompromised host: CD4-helper-independent antiviral function of CD8-positive memory T lymphocytes derived from latently infected donors. J. Virol. **62:**1061–1065.
38. **Reddehase, M. J., W. Mutter, and U. H. Koszinowski.** 1987. In vivo application of recombinant interleukin 2 in the immunotherapy of established cytomegalovirus infection. J. Exp. Med. **165:**650–656.
39. **Reddehase, M. J., F. Weiland, K. Münch, S. Jonjic, A. Lüske, and U. H. Koszinowski.** 1985. Interstitial murine cytomegalovirus pneumonia after irradiation: characterization of cells that limit viral replication during established infection of the lungs. J. Virol. **55:**264–273.
40. **Riddell, S. R., K. S. Watanabe, J. M. Goodrich, C. R. Li, M. E. Agha, and P. D. Greenberg.** 1992. Restoration of viral immunity in immunodeficient humans by the adoptive transfer of T cell clones. Science **257:**238–241.
41. **Rubocki, R. J., T. H. Hansen, and D. R. Lee.** 1986. Molecular studies of murine mutant BALB/c-H-2-dm2 define a deletion of several class I genes including the entire H-2Ld gene. Proc. Natl. Acad. Sci. USA **83:**9606–9610.
42. **Russell, E. S.** 1979. Hereditary anemias of the mouse: a review for geneticists. Adv. Genet. **20:**357–459.
43. **Scalzo, A. A., N. A. Fitzgerald, A. Simmons, A. B. La Vista, and G. A. Shellam.** 1990. Cmv-1, a genetic locus that controls murine cytomegalovirus replication in the spleen. J. Exp. Med. **171:**1469–1483.
44. **Shaklai, M.** 1989. Cellular components of stroma in vivo in comparison with in vitro systems, p. 219–251. *In* M. Tavassoli (ed.), Handbook of the hematopoietic microenvironment. Humana Press, Clifton, N.J.
45. **Shirai, A., K. Holmes, and D. Klinman.** 1993. Detection and quantitation of cells secreting IL-6 under physiologic conditions in BALB/c mice. J. Immunol. **150:**793–799.
46. **Simmons, P., K. Kaushansky, and B. Torok-Storb.** 1990. Mechanisms of cytomegalovirus-mediated myelosuppression: perturbation of stromal cell function versus direct infection of myeloid cells. Proc. Natl. Acad. Sci. USA **87:**1386–1390.
47. **Sredni, B., Z. Rosenthal-Galili, H. Michlin, D. Sobelman, Y. Seger, S. Blagerman, Y. Kalechman, and B. Rager-Zisman.** 1994. Restoration of murine cytomegalovirus (MCMV) induced myelosuppression by AS101. Immunol. Lett. **43:**159–165.
48. **Tsuchiya, M., S. Asano, Y. Kaziro, and S. Nagata.** 1986. Isolation and characterization of the cDNA for murine granulocyte colony-stimulating factor. Proc. Natl. Acad. Sci. USA **83:**7633–7637.
49. **Weiland, F., G. M. Keil, M. J. Reddehase, and U. H. Koszinowski.** 1986. Studies on the morphogenesis of murine cytomegalovirus. Intervirology **26:** 192–201.
50. **Williams, D. E., P. de Vries, A. E. Namen, M. B. Widmer, and S. D. Lyman.** 1992. The Steel factor. Dev. Biol. **151:**368–376.
51. **Yuhasz, S. A., V. B. Dissette, M. L. Cook, and J. G. Stevens.** 1994. Murine cytomegalovirus is present in both chronic active and latent states in persistently infected mice. Virology **202:**272–280.
52. **Zsebo, K. M., D. A. Williams, E. N. Geissler, V. C. Broudy, F. H. Martin, H. L. Atkins, R. Y. Hsu, N. C. Birkett, K. H. Okino, D. C. Murdock, F. W. Jacobsen, K. E. Langley, K. A. Smith, T. Takeishi, B. M. Cattanach, S. J. Galli, and S. V. Suggs.** 1990. Stem cell factor is encoded at the SI locus of the mouse and is the ligand for the c-kit tyrosine kinase receptor. Cell **63:**213–224.